



**HAL**  
open science

## Two-dimensional nonlinear modes and frequency combs in bottle microresonators Letter

Y. V. Kartashov, M. L Gorodetsky, Alexandre Kudlinski, D. V. Skryabin

► **To cite this version:**

Y. V. Kartashov, M. L Gorodetsky, Alexandre Kudlinski, D. V. Skryabin. Two-dimensional nonlinear modes and frequency combs in bottle microresonators Letter. *Optics Letters*, 2018, 43 (11), pp.2680-2683. 10.1364/OL.43.002680 . hal-02964269

**HAL Id: hal-02964269**

**<https://hal.science/hal-02964269>**

Submitted on 15 Oct 2020

**HAL** is a multi-disciplinary open access archive for the deposit and dissemination of scientific research documents, whether they are published or not. The documents may come from teaching and research institutions in France or abroad, or from public or private research centers.

L'archive ouverte pluridisciplinaire **HAL**, est destinée au dépôt et à la diffusion de documents scientifiques de niveau recherche, publiés ou non, émanant des établissements d'enseignement et de recherche français ou étrangers, des laboratoires publics ou privés.

# Two-dimensional nonlinear modes and frequency combs in bottle microresonators

Y. V. KARTASHOV,<sup>1,2,\*</sup> M. L. GORODETSKY,<sup>3,4</sup> A. KUDLINSKI,<sup>5</sup> AND D. V. SKRYABIN<sup>2,3,6</sup>

<sup>1</sup>Institute of Spectroscopy, Russian Academy of Sciences, Troitsk, Moscow 108840, Russia

<sup>2</sup>Department of Physics, University of Bath, Bath BA2 7AY, UK

<sup>3</sup>Russian Quantum Center, Skolkovo 143025, Russia

<sup>4</sup>Faculty of Physics, Lomonosov Moscow State University, Moscow 119991, Russia

<sup>5</sup>Université Lille, CNRS, UMR 8523-PhLAM-Physique des Lasers Atomes et Molécules, F-59000 Lille, France

<sup>6</sup>ITMO University, St. Petersburg 197101, Russia

\*Corresponding author: Yaroslav.Kartashov@icfo.eu

Received 27 March 2018; accepted 26 April 2018; posted 7 May 2018 (Doc. ID 326985); published 31 May 2018

**We theoretically investigate frequency comb generation in a bottle microresonator accounting for the azimuthal and axial degrees of freedom. We first identify a discrete set of the axial nonlinear modes of a bottle microresonator that appear as tilted resonances bifurcating from the spectrum of linear axial modes. We then study azimuthal modulational instability of these modes and show that families of two-dimensional (2D) soliton states localized both azimuthally and axially bifurcate from them at critical pump frequencies. Depending on detuning, 2D solitons can be stable, form persistent breathers or chaotic spatio-temporal patterns, or exhibit collapse-like evolution.** © 2018 Optical Society of America

**OCIS codes:** (140.3945) Microcavities; (190.5940) Self-action effects.

<https://doi.org/10.1364/OL.43.002680>

Whispering gallery mode microresonators are known to generate Kerr frequency combs when a sufficiently strong external pump is tuned into a resonance with one of the azimuthal modes of the resonator. Such frequency combs can be used in a number of applications, including precision spectroscopy and optical signal processing; see, e.g., Refs. [1–3]. A particularly important frequency comb state is the one where either one or several solitons are generated as a result of the phase locking of a large number of different azimuthal modes. The demonstration of soliton combs in microresonators in both anomalous [4,5] and normal [6] dispersion regimes has been a crucial step towards realization of compact solid-state sources of tunable broadband combs. Frequency combs in relatively long and thin microrings are accurately described by the one-dimensional (1D) Lugiato–Lefever (LL) model [7–10], where a single spatial dimension corresponds to the azimuthal coordinate along the resonator circumference. This model is derived and valid under an assumption that the transverse modal structure related to two remaining spatial degrees of

freedom is frozen. Experimental situations, where coupling between several azimuthal families of modes corresponding to different transverse field profiles impacts comb generation and soliton formation processes in microrings, are also known; see, e.g., Ref. [11]. An interplay between several spatial degrees of freedom can also be considered in other types of microresonators such as bottle [12–15], spherical/spheroidal [16–18], and microbubble [19,20]. An important feature of those is that ratios between free-spectral ranges (FSRs) associated with different modal families can be more readily controlled here [15,18]. This opens new opportunities for generation of tunable frequency combs and observation of a wide spectrum of other nonlinear phenomena [15,17,18]. Considering bottle resonators, two groups have recently developed a theory of frequency comb generation in them that has used a 1D LL model with parabolic potential, and demonstrated multistability [19] and frequency comb generation [21,22] effects relying on the axial mode family.

In this Letter, we consider the generation of two-dimensional (2D) frequency combs in bottle microresonators, taking into account dynamics in the axial and azimuthal directions. In particular, we address a practically relevant geometry [15] where the azimuthal FSR exceeds the axial one by a couple of orders of magnitude, so that the corresponding resonator spectrum consists of clusters of the axial modes attached to the well-separated azimuthal modes. We found 2D soliton solutions that bifurcate from the nonlinear axial modes. When these solitons destabilize through the change of the pump frequency, they transform into breathers, decay, or exhibit quasi-collapses.

We describe the dimensionless field envelope function  $\Psi$  in a bottle microresonator proposing a 2D generalization of the 1D Lugiato–Lefever equation used in Refs. [21,22] to describe combs in bottle resonators. Our model takes into account an axial ( $Z$  direction) trapping potential and pump localization, as well as the dependence on the azimuthal coordinate  $\theta$  corresponding to the whispering gallery modes rotating around the bottle axis:

$$i\partial_T \Psi = -\frac{1}{2} d \partial_Z^2 \Psi + \omega_0 \Psi - i \mathcal{D}_1 \partial_\theta \Psi - \frac{1}{2} \mathcal{D}_2 \partial_\theta^2 \Psi + \frac{f^2}{2d} \mathcal{U}(Z) \Psi - i \kappa \Psi - f \Psi |\Psi|^2 - f \mathcal{H}(Z) e^{-i\omega_p T}, \quad (1)$$

where  $T$  is the physical time,  $\kappa$  is the loss rate, and  $\omega_p$  is the pump frequency. An integrated dispersion in the azimuthal direction is approximated by  $\mathcal{D}_1 \mu + \mathcal{D}_2 \mu^2/2$ , where  $\mu$  is the azimuthal mode index,  $\mathcal{D}_1/2\pi$  is the azimuthal FSR, and  $\mathcal{D}_2$  is the second-order azimuthal dispersion. Scaling for  $\Psi$ , potential  $\mathcal{U}$  and pump  $\mathcal{H}$  are chosen in a way that the parameter  $f/2\pi$  yields the axial FSR. Indeed, the linear and pump-free spectrum of Eq. (1) obtained by substituting  $\Psi \sim \psi_{\nu\mu} \exp(-i\omega_{\nu\mu} T - i\mu\theta)$  and assuming a parabolic trapping potential,  $\mathcal{U} = Z^2$ , reads as  $\omega_{\nu\mu} - \omega_0 = f(\nu + 1/2) + \mu \mathcal{D}_1 + \mu^2 \mathcal{D}_2/2$ , where  $\nu$  is the axial index and  $\psi_{\nu\mu}$  are the eigenmodes of the harmonic oscillator. Thus, the spectrum is equidistant in  $\nu$ , and  $f$  is the distance between the resonances. If a bottle microresonator has an axial length  $L$ , a core radius  $r$ , and an axial curvature  $R$  [21,23], then the azimuthal and axial FSRs  $\mathcal{D}_1 \approx c/n_0 r$  and  $f \approx c/n_0 (rR)^{1/2}$ . We set  $\Psi = \psi \exp(-i\omega_p T)$  and introduce dimensionless time  $t = fT$  and coordinate  $z = f^{1/2} Z/d^{1/2}$  to get a dimensionless equation:

$$i\partial_t \psi = -\frac{1}{2} \partial_z^2 \psi + (\delta - i\beta_1 \partial_\theta - \beta_2 \partial_\theta^2) \psi + \frac{\mathcal{U}(z)}{2} \psi - i\gamma \psi - \psi |\psi|^2 - \mathcal{H}(z), \quad (2)$$

with detuning  $\delta = (\omega_0 - \omega_p)/f$ , losses  $\gamma = \kappa/f$ , and dispersion coefficients  $\beta_1 = \mathcal{D}_1/f$  and  $\beta_2 = \mathcal{D}_2/2f$ . We assume that the resonator is pumped through an optical fiber running transverse to the bottle axis, which corresponds to the well-localized  $\mathcal{H} = b \exp[-(z - z_p)^2/w^2]$ , where  $w$  is the pump width ( $w = 0.2$  in what follows), and  $z_p$  is the pump position relative to the resonator center. Accounting for spatial localization of the pump is important for spectrally dense modal families, where FSR is comparable to the nonlinear shifts of the resonances and can be disregarded for the ones with the relatively large FSRs [24]. For a microresonator with a radius  $r = 1$  mm, a curvature  $R = 100$  m, and a length  $L = 2.2$  mm, one obtains  $\mathcal{D}_1 = 200$  GHz,  $f = 0.6$  GHz. Such resonator supports about  $N = 50$  axial modes. To account for the finite bottle, we set  $\mathcal{U} = 2N$  for  $|z| > (2N)^{1/2}$ . In what follows, we use  $\gamma = 0.004$ , giving the linewidth  $\kappa = 2.4$  MHz and  $\beta_2 = 0.1$  corresponding to  $\mathcal{D}_2 \approx 120$  MHz. Equation (2) was solved with the boundary conditions  $\psi(z, \theta) = \psi(z, \theta + 2\pi)$  and  $\psi(z \rightarrow \infty, \theta) = 0$ .

We first consider solutions of Eq. (2) that are uniform in  $\theta$ , physically corresponding to the azimuthal structure of a whispering gallery mode with the frequency nearest to the pump frequency. Varying the detuning parameter, we build a family of the axial modes peaking at  $\delta = -(\nu + 1/2)$  and shaping a set of tilted nonlinear resonances [see Figs. 1(a) and 1(b) showing the peak amplitude  $|\psi|_{\max}$  of the nonlinear modes as a function of  $\delta$ ]. When the resonator is pumped exactly at the center ( $z_p = 0$ ), then only even modes with the axial indices  $\nu = 0, 2, \dots$  are excited [Fig. 1(a)]. Examples of 1D profiles of such modes can be found in Ref. [21]. Resonances are tilted and may overlap, creating a multistability situation. The overlap of the central pump with the higher-order harmonic oscillator modes reduces with the increase of  $\nu$  and, hence, resonance peaks gradually decrease with  $\delta$ ; see Fig. 1(a). If pump is shifted to the intensity maximum of one of the higher-order modes,

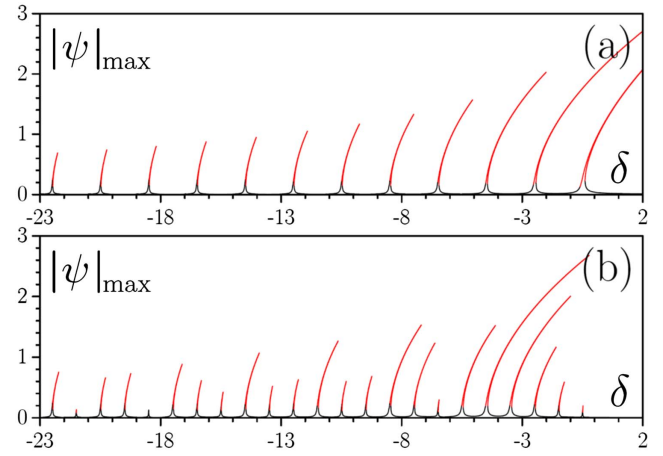


**Fig. 1.** Set of resonance curves corresponding to the family of nonlinear axial modes with the azimuthal index  $m = 0$ . (a)  $z_p = 0$  and (b)  $z_p = 2.417$ . Here and in all figures,  $b = 0.08$  and  $\gamma = 0.004$ .

for example to  $z_p = 2.417$  (maximum of the  $\nu = 4$  mode), then the tilted resonances are found for odd and even modes and the modes around  $\nu = 4$  are excited most efficiently; see Fig. 1(b).

Families of solutions shown in Fig. 1 can be subject to the instability development stimulated by small  $\theta$ -dependent perturbations. To analyze this effect, we use an ansatz  $\psi(z) + u(z)e^{\lambda t + im\theta} + v^*(z)e^{\lambda^* t - im\theta}$ , where  $m$  is the azimuthal index, and  $\lambda$  is the perturbation growth rate. Linearizing Eq. (2), we find the following eigenvalue problem:

$$\begin{aligned} i\lambda u &= (\delta + \beta_1 m + \beta_2 m^2 + \mathcal{U}/2 - i\gamma - 2|\psi|^2 - \partial_z^2/2)u - \psi^2 v, \\ i\lambda v &= \psi^* u - (\delta - \beta_1 m + \beta_2 m^2 + \mathcal{U}/2 + i\gamma - 2|\psi|^2 - \partial_z^2/2)v. \end{aligned} \quad (3)$$

Solving it numerically, we find a typical modulational instability band structure (see Fig. 2) that exists for all the upper branches of all the tilted resonances. The instability bandwidth decreases monotonically with the increase of the axial mode index  $\nu$  for  $z_p = 0$ , and it varies nonmonotonically with  $\nu$  for the off-center pump acquiring maximal values for the strongest resonances. Unstable axial modes are indicated with the red full lines in Figs. 1 and 3. The instability of the upper branches around resonances was encountered for a broad range of  $b, \gamma$  values. The instability typically breaks these modes into

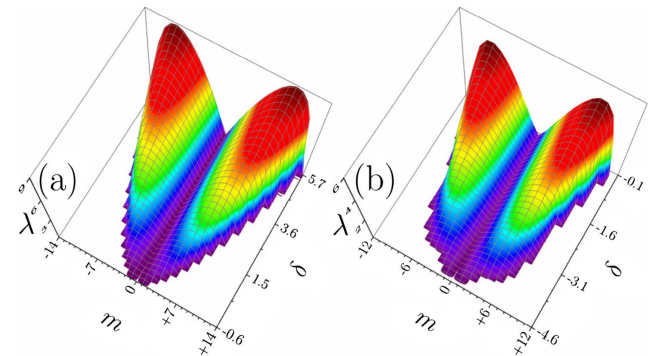


**Fig. 2.** Modulational instability growth rate calculated for (a) the axial mode with  $\nu = 0$  and  $z_p = 0$ , and (b)  $\nu = 5$  and  $z_p = 2.417$ .

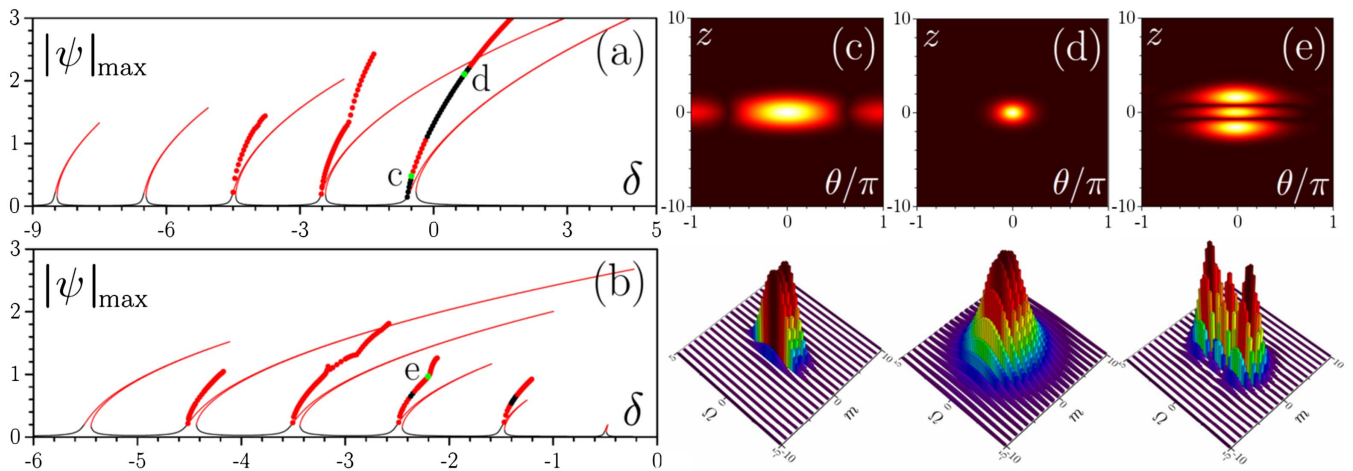


**Fig. 3.** (a), (b) Full lines show nonlinear resonances as in Figs. 1(a) and 1(b). The dots show peak amplitudes  $|\psi|_{\max}$  of the 2D solitons. Stable/unstable solutions are shown in black/red. (c)–(e) Examples of the real and frequency space profiles of the 2D solitons corresponding to points **c**, **d**, and **e** in (a) and (b).

a complex pattern consisting of multiple solitons, sometimes with different axial structures, rotating around the bottle axis.

To isolate and study the rotating 2D solitons, we search for 2D nonlinear modes of Eq. (2) in a moving coordinate frame, where the term  $\sim \beta_1 \partial_\theta \psi$  is eliminated:  $\psi(t, \theta, z) \rightarrow \psi(t, \theta', z)$  and  $\theta' = \theta - \beta_1 t$ . We found that families of these solitons bifurcate from the upper branches of the axial modes exactly at the detuning values, where the latter become modulationally unstable; see Figs. 3(a) and 3(b). The azimuthal solitons that we found inherit an axial structure corresponding to the respective axial modes. Close to the bifurcation point, they are delocalized in  $\theta$ , while they rapidly narrow down when detuning increases; see Figs. 3(c) and 3(d). This is accompanied by substantial expansion of the spectrum in both axial ( $\Omega$ ) and azimuthal ( $m$ ) directions. This is particularly notable in the azimuthal direction, since the azimuthal spectrum is effectively a single mode at a bifurcation point. Examples of azimuthal spectra calculated using field distributions  $\psi(\theta, z = 0)$  in the center of resonator ( $z = 0$ ) are shown in Fig. 4. While solitons bifurcating from the modes with relatively small values of the axial index  $\nu$  are localized very well, the ones with many axial intensity oscillations ( $\nu > 2$ ) typically acquire complex background in the azimuthal direction with an increase of  $\delta$ . It was unfeasible to trace all possible soliton families due to multiple bifurcations corresponding to solutions with a more complex azimuthal structure.

However, the simplest families are shown in Fig. 3. The results presented in Fig. 3 constitute the first example of 2D comb solitons. We analyzed the stability of 2D comb solitons by solving Eq. (2) directly with slightly perturbed soliton inputs

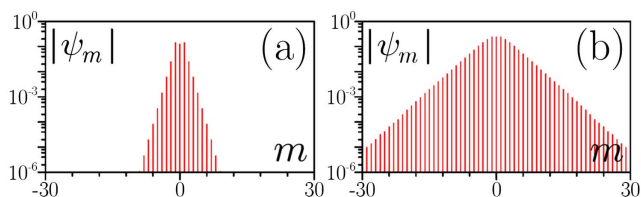


**Fig. 4.** Azimuthal spectra at (a)  $\delta = -0.5$  and (b)  $\delta = 0.7$  calculated in the point  $z = 0$  and corresponding to points **c** and **d** in Fig. 3(a).

up to evolution times exceeding  $t = 10^4$ . Stable 2D soliton branches are marked black, while unstable branches are shown in red. In the case of the central pump, we found a sufficiently broad interval of frequency detuning where 2D solitons connecting to the ground state of the harmonic oscillator,  $\nu = 0$ , are stable. The off-centered pump provides only very narrow intervals of stability for 2D solitons connected to the  $\nu = 1$  and  $\nu = 2$  states of the harmonic oscillator that are stable in narrow detuning intervals.

Unstable solitons have been found to demonstrate diverse spatio-temporal dynamics. For example, we have observed that the  $\nu = 2$  solitons for  $z_p = 0$  transform into persistent breathers; see Fig. 5. Note that this transformation is accompanied by minimal modifications of the soliton spectrum and by the

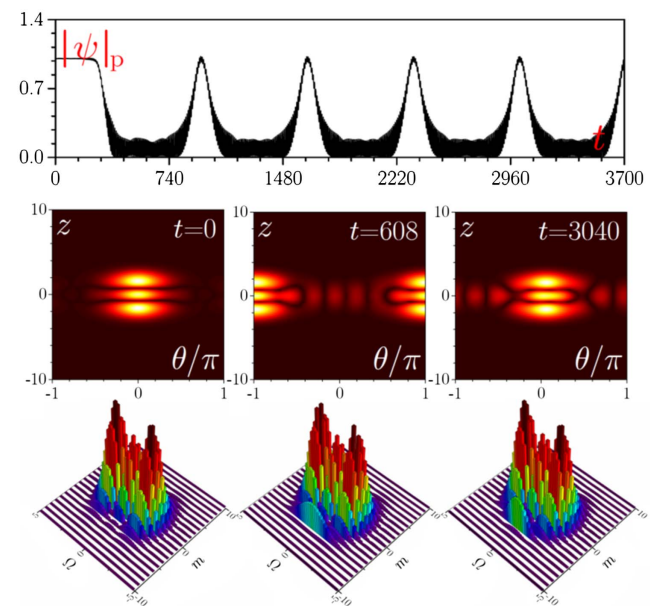


**Fig. 5.** 2D breather soliton around the  $\nu = 2$  axial mode for  $\delta = -2.1$  and  $z_p = 0$ . Top row, field amplitude at  $\theta = 0, z = z_p$ ; middle and bottom rows, real and frequency space distributions for different moments of time.

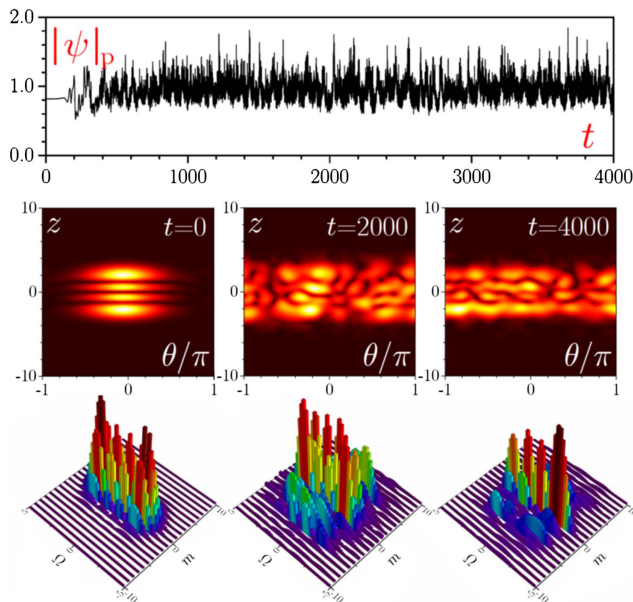


**Fig. 6.** Chaotic spatio-temporal dynamics emerging from the instability of the 2D soliton around the  $\nu = 3$  axial mode for  $\delta = -3.3$  and  $z_p = 2.417$ . The arrangement of the panels is the same as in Fig. 5.

accumulation of the velocity offset in the azimuthal direction. To make this offset visible, in Fig. 5 we eliminated the  $\beta_1 \partial_\theta \psi$  terms corresponding to the fast soliton rotation. The small variation of FSR arising due to this offset can be estimated as  $2\pi/T_b$ , where  $T_b$  is the time interval between the subsequent peaks in Fig. 5, corresponding to the arrival of the moving breather to the  $\theta, z_p = 0$  point. Notice that, in addition to velocity offset, the breather also exhibits small periodic oscillations of peak amplitude. The most common instability scenario for modes with large axial indices  $\nu$  is the initial contraction followed by fragmentation of the profile into a pattern of random filaments. These chaotic patterns either persist for a very

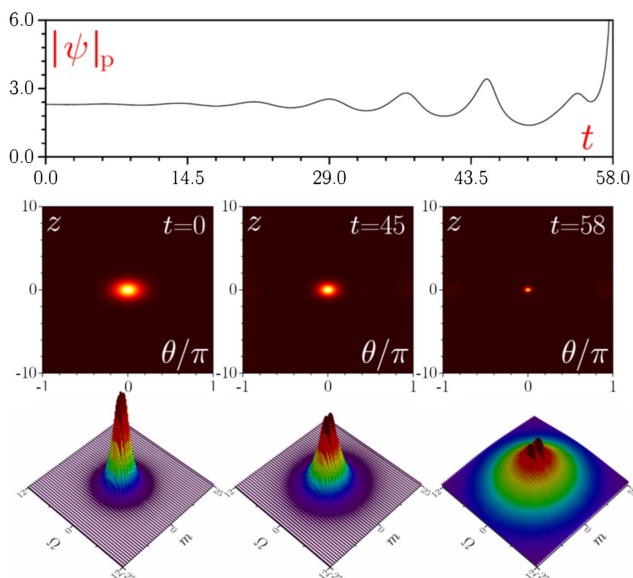


**Fig. 7.** Collapse of the unstable  $\nu = 0$  soliton at  $\delta = 0.9$  and  $z_p = 0$ .

long time (see Fig. 6) or evolve into a stable nonlinear mode corresponding to the low amplitude branch of the tilted resonances. Another instability scenario of 2D solitons, which occurs when their amplitude becomes sufficiently large, is the soliton collapse which is accompanied not only by a dramatic narrowing of the field profile in both coordinates, but also by a pronounced spectral broadening in both axial and azimuthal frequencies (Fig. 7). Collapse is of course an unphysical effect and is expected to be arrested through the inclusion of the higher-order dispersive terms into the model equation, which should be a subject of future research.

**Funding.** Russian Science Foundation (RSF) (17-12-01413); Leverhulme Trust (RPG-2015-456); Government of Russian Federation (074-U01); EU H2020 (691011-SOLIRING).

**Acknowledgment.** D. Skryabin acknowledges the ITMO University Visiting Professorship Scheme via the Government of Russian Federation. D. Skryabin and M. Gorodetsky acknowledge EU H2020 for exchange visits. D. Skryabin and Y. Kartashov acknowledge support from the Leverhulme Trust.

## REFERENCES

1. T. J. Kippenberg, R. Holzwarth, and S. A. Diddams, *Science* **332**, 555 (2011).
2. J. Pfeifle, V. Brasch, M. Lauer, Y. Yu, D. Wegner, T. Herr, K. Hartinger, P. Schindler, J. S. Li, D. Hillerkuss, R. Schmogrow, C. Weimann, R. Holzwarth, W. Freude, J. Leuthold, T. J. Kippenberg, and C. Koos, *Nat. Photonics* **8**, 375 (2014).
3. M. G. Suh and K. J. Vahala, *Science* **359**, 884 (2018).
4. T. Herr, V. Brasch, J. D. Jost, C. Y. Wang, N. M. Kondratiev, M. L. Gorodetsky, and T. J. Kippenberg, *Nat. Photonics* **8**, 145 (2014).
5. X. Yi, Q. F. Yang, K. Y. Yang, M. G. Suh, and K. Vahala, *Optica* **2**, 1078 (2015).
6. X. Xue, Y. Xuan, Y. Liu, P.-H. Wang, S. Chen, J. Wang, D. E. Leaird, M. Qi, and A. M. Weiner, *Nat. Photonics* **9**, 594 (2015).
7. L. A. Lugiato and R. Lefever, *Phys. Rev. Lett.* **58**, 2209 (1987).
8. S. Coen, H. G. Randle, T. Sylvestre, and M. Erkintalo, *Opt. Lett.* **38**, 37 (2013).
9. Y. K. Chembo and C. R. Menyuk, *Phys. Rev. A* **87**, 053852 (2013).
10. C. Milián, A. V. Gorbach, M. Taki, A. V. Yulin, and D. V. Skryabin, *Phys. Rev. A* **92**, 033851 (2015).
11. T. Herr, V. Brasch, J. D. Jost, I. Mirgorodskiy, G. Lihachev, M. L. Gorodetsky, and T. J. Kippenberg, *Phys. Rev. Lett.* **113**, 123901 (2014).
12. M. Pollinger, D. O'shea, F. Warken, and A. Rauschenbeutel, *Phys. Rev. Lett.* **103**, 053901 (2009).
13. M. Pollinger and A. Rauschenbeutel, *Opt. Express* **18**, 17764 (2010).
14. M. Sumetsky, *Phys. Rev. Lett.* **111**, 163901 (2013).
15. V. Dvoyrin and M. Sumetsky, *Opt. Lett.* **41**, 5547 (2016).
16. M. Gorodetsky, *Optical Microresonators with Gigantic Quality Factor* (Fizmatlit, 2011).
17. K. E. Webb, M. Erkintalo, S. Coen, and S. G. Murdoch, *Opt. Lett.* **41**, 4613 (2016).
18. A. A. Savchenkov, A. B. Matsko, W. Liang, V. S. Ilchenko, D. Seidel, and L. Maleki, *Nat. Photonics* **5**, 293 (2011).
19. D. Farnesi, A. Barucci, G. C. Righini, G. N. Conti, and S. Soria, *Opt. Lett.* **40**, 4508 (2015).
20. Q. Lu, S. Liu, X. Wu, L. Liu, and L. Xu, *Opt. Lett.* **41**, 1736 (2016).
21. I. Oreshnikov and D. V. Skryabin, *Opt. Express* **25**, 10306 (2017).
22. S. V. Suchkov, M. Sumetsky, and A. A. Sukhorukov, *Opt. Lett.* **42**, 2149 (2017).
23. Y. A. Demchenko and M. L. Gorodetsky, *J. Opt. Soc. Am. B* **30**, 3056 (2013).
24. Y. V. Kartashov, O. Alexander, and D. V. Skryabin, *Opt. Express* **25**, 11550 (2017).